HIGH RESOLUTION DIGITAL IMAGE CORRELATION STRAIN MEASUREMENTS OF ADHESIVELY BONDED JOINTS

J. Kosmann[1], T. Löbel[1,2], D. Holzhüter[1,3], C. Hühne[1, 4] and M. Schollerer[1,5]

[1]Institute of Composite Structures and Adaptive System, Department of Composite Design, German Aerospace Center, Lilienthalplatz 7, 38108 Braunschweig, Germany
[1]Email: jens.kosmann@dlr.de, Web Page: http://www.dlr.de/fa
[1]Email: jens.kosmann@dlr.de,
[2]Email: thomas.loebel@dlr.de,
[3]Email: dirk.holzhueter@dlr.de,
[5]Email: martin.schollerer@dlr.de,
[4]Institute of Adaptronic and Functional Integration, TU-Braunschweig, Langer Kamp 6, 38106 Braunschweig, Germany
[1]Email: Christian.huehne@dlr.de, Web Page: https://www.tu-braunschweig.de/iaf

Keywords: Scarf repair, tension testing, Crack Lap Shear, bonding, optical measurement, ARAMIS, Digital image correlation

Abstract

The focus of the work presented is the high resolution digital image correlation strain measurement of adhesively bonded joints. Especially in scarf repaired coupons and crack lap shear specimens the strain distribution along the bondline is highly uneven. This cannot be covered by single measuring points like strain gauges. Therefore the optical strain measurement system ARAMIS is used which is based on the digital image correlation method. With digital image correlation it is possible to gain detailed strain information over the complete measurement area. In this paper the challenge is to find the right combination of lenses. Test setup and the right surface treatment especially for small measurement volumes are analyzed and discussed. The aim is to use the full resolution of 12 mega pixel for the measurement area around the bondline. This possibility in combination with a suitable surface treatment allows a detailed view on the adhesive layer. The results allow detailed visualization of the strain distribution. Comparisons to Finite Element simulations are shown and discussed. Additionally to scarf joints, the examinations are extended to a crack lap joint configuration.

1. Introduction

In tensile test setups strain gauges or extensometers are typically used to measure the strain. Strain gauges and extensometers provide average values over the size of the strain gauges or distance between the measurement points but no information for the remaining area of the specimen. This is reasonable for monolithic isotropic materials with small deformations. However for anisotropic materials, like composites or bonded joints, the average values may not be sufficient. Important strain deviations may not be detected. Detailed quantitative strain measurements are important to understand the specimen and validate FE Models. Therefore different optical methods are possible. Mollenhauer

Excerpt from ISBN 978-3-00-053387-7

et.al [1] using the moiré interferometry for a full-field optical displacement measuring. For the technique a grating on the surface is necessary. Within this paper the digital image correlation (DIC) method is used to get a full field optical displacement measurement. As digital image correlation (DIC) systems are measuring the displacement on the top surface of the specimen, coupon specimens have the advantage of free edges where the scarf and the adhesive layer are visible. Spaggiari et. al. [2] for example using the DIC method to measure the shear strength of structural adhesives.

For this paper three different types of specimens and two different measurement setups are considered. The main focus is on scarf repaired coupon specimens in pristine conditions as well as specimens with intended bondline flaws. The third specimens are Crack Lap joint configurations where the highly loaded overlap edges are investigated since they are most critical for the overall joint failure. These results are relevant to validate FEM simulations and help to optimize adhesively bonded joints.

The materials used within this work are laminates made of carbon fiber reinforced epoxide prepreg systems (CFRP) and epoxide film adhesive. The specimens have a quasi-isotropic 24 plies stacking. Each single ply has a cured thickness of 0.13mm. The adhesive has a thickness of 0,1mm. For scarf repaired specimens a scarf ratio of 1:20 is used. In the analytical calculation of the bondline strain for the scarfed bonded joint the highly uneven strain distribution becomes visible. Due to the different fiber orientations each ply has a different effect and may causes strain peaks in the bondline.

The aim is to measure the strain within the bondline and within single plies. Due to the thin CRFP plies and the thin adhesive the measuring resolution needs to be less than 0,1mm. Therefore the high resolution DIC ARAMIS 12M system from GOM is used. The ARAMIS system can be used either as a 2D DIC system with only one camera to detect in-plane displacements or as a 3D DIC system using two cameras and triangulation procedure to detect out of plane displacements also. The calibration of a 3D setup allows the evaluation of quantitative results. In this paper 2D as well as 3D setups are used depending on the measurement area.

2. ARAMIS System

To measure with DIC System different parameters have to be defined. This chapter focusses on the setup parameter to achieve the intended measurement volume and resolution. Therefore different surface preparations are necessary. The post processing after the measurement is also discussed.

2.1 Parameters for the ARAMIS Setup

To set up the ARAMIS system several parameters need to be defined. The first question is if it should be a 2D or a 3D setup. For larger measurement volumes the 3D setup has advantages as it is a calibrated system and out of plane deformations are detected. But especially for the extremely small measurement volumes, smaller then 15mm x 10mm, the depth of focus is too small for a 3D setup. Here a 2D setup has the advantage that the camera looks perpendicular on the specimen.

After the definition of the measurement volume the focus of the lens is selected. To set the right zoom factor, distance rings are mounted between lenses and sensor. For 3D setups, see Figure 1 (left), the slider distance S is defined that both cameras view the same point under a defined camera angle α and measuring distance D.

To illuminate the measurement area a monochromatic polarized blue LED light projector, see Figure 1 (right) is used. The lenses of the cameras are equipped with circular polarizing filters, to reduce reflections. The aim is to close the aperture and minimize the shutter speed at the same time. A small

Excerpt from ISBN 978-3-00-053387-7

aperture is necessary to get a sufficient depth of focus. A short shutter time reduces the risk of camera shake.

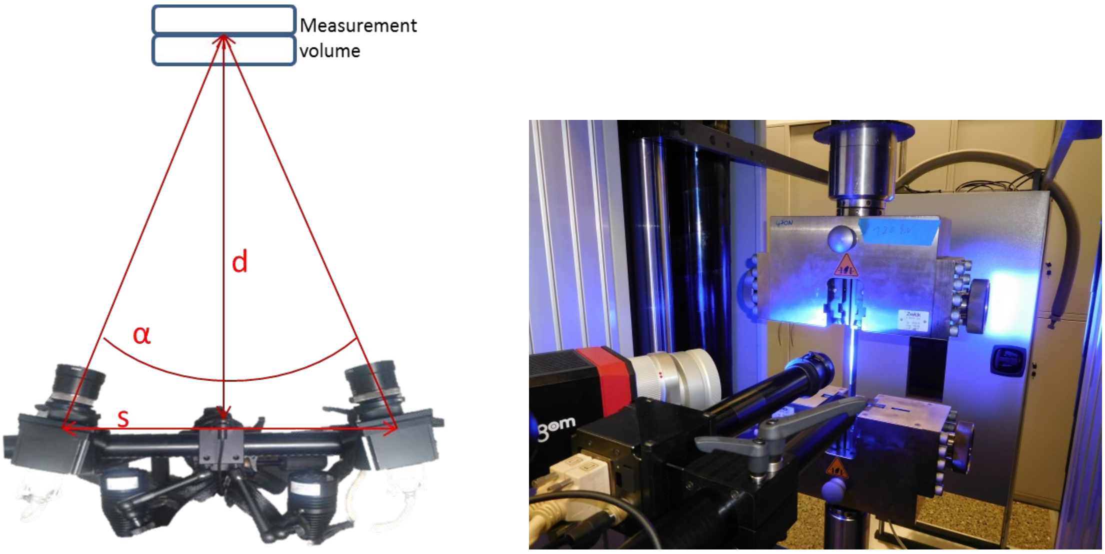

Figure 1: Parameters of a 3D setup (left) and 2D setup with illumination (right)

2.2 Measurement Volume and Theoretical Resolution

Bevor the definition of the system parameters, the desired measurement volume is defined. Depending on the measurement area the resolution varies. The larger the measurement area the worse is the local resolution.

For measuring the strain distribution within the bondline a high local measuring resolution is necessary. Because of the different effects of each ply orientation on the strain in the bondline it is necessary to measure at least one ply of each direction in the scarf. With the used stacking and the scarf ratio of 1:20 this means that at least 4 plies have to be measured, also the displacement of specimen and clamping, during testing has to be considered. As in Figure 2 shown, this is resulting in a measurement volume length of at least 12mm. Based on this and the given 12 mega pixel resolution with a ratio of 4:3 the optical size of one pixel is calculated.

$$\frac{12\text{ mm}}{4096\text{ pixel}} \text{ x } \frac{9\text{ mm}}{3072\text{ pixel}} \approx 0{,}003^2 \frac{\text{mm}^2}{\text{pixel}}. \tag{1}$$

For calculation of the facets each facet needs to have at least some dark and bright spots within its area. Therefore a suitable minimum size is 10 x 10 pixels. But to increase the robustness against voids in the speckle pattern the facet size should be increased.

$$10\text{pixel}\frac{0.003\text{ mm}}{\text{pixel}} \text{ x } 10\text{pixel}\frac{0.003\text{ mm}}{\text{pixel}} \approx 0.03\text{mm x } 0.03\text{ mm}. \tag{2}$$

0.03mm x 0.03mm is the measurement area of one facet. Due to the overlap of two facets which is set to 4 pixels, the minimum pixel area for a strain calculation is 22 x 22 pixels which is equivalent to

Excerpt from ISBN 978-3-00-053387-7

0.066mm x 0.066mm. This means that every 0,03mm one measuring point exist which is the average over an area of 0.0044mm². As the bondline thickness is 0,1mm the resolution of the system is sufficient.

To achieve a measurement area of 12 x 9 mm, the lenses need to enhance the specimen on the camera sensor (36 x 24mm). For this setup a 100mm focal lens with 21cm distance rings are used. But with this magnification, the depth of focus is too small for a 3D setup, thus a 2D setup is used.

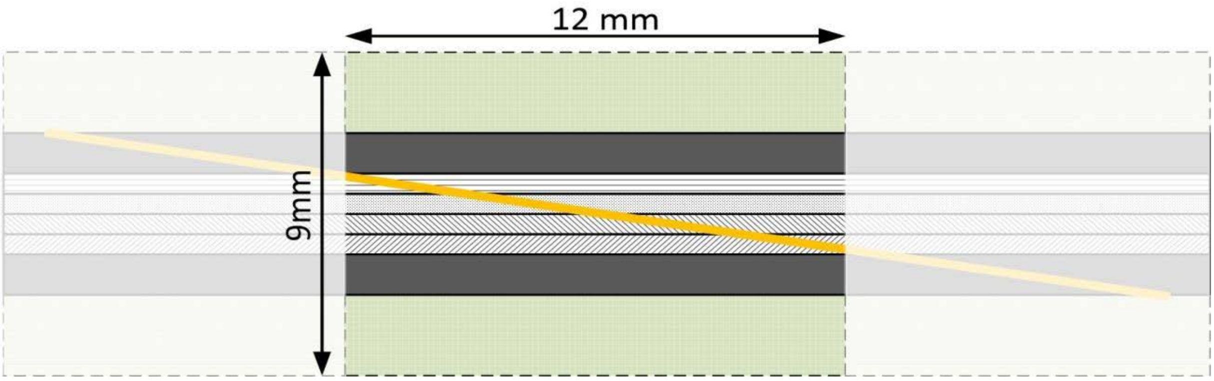

Figure 2: smallest Measurement volume to measure 4 plies in scarfed repair

2.3 Preparation of Speckle Pattern

Once the measurement volume is defined a suitable preparation of the specimen's surface is the next key factor. The quality of the speckle painting determines the possible resolution of DIC measurements. The speckles are a stochastic pattern of dots randomly distributed over a monochrome surface. The speckles should have a high contrast. The size is depends on the measurement area.

Different surface preparation processes can be used depending on the size of the measurement area. In this case the focus is on measuring small areas. Figure 3 shows different techniques of preparing the pattern with different paints. For the described setup one facet has an area of 0.03mm x 0.03mm. Within this area white and dark speckles have to be enclosed.

Different lacquer techniques are investigated to produce an optimal and repeatable speckle painting. Three different systems are investigated. The result is plotted in Figure 3. The first (left) is a white powder background combined with a black graphite spray. Both painted with an aerosol can. The microscope shows speckles in the range of 60 to 170µm but also big gaps. Furthermore reproducibility is not given. The second system (middle) is a combination of white and black modeling paint. The painting has a good contrast but due to the surface tension of the paint big gaps between the speckles occur. System three (right) is a combination of white titanium dioxide and black iron oxide powder which is dispersed in ethanol. This combination has a uniform speckle pattern with an average size of 27µm. This as well as the modeling paint system are lacquered with an airbrush system and allow repeatable speckle patterns. The uniform stochastic speckle and the repeatability of the titanium dioxide and black iron oxide system provides the best surface preparation, at least for the small measurement areas.

Excerpt from ISBN 978-3-00-053387-7

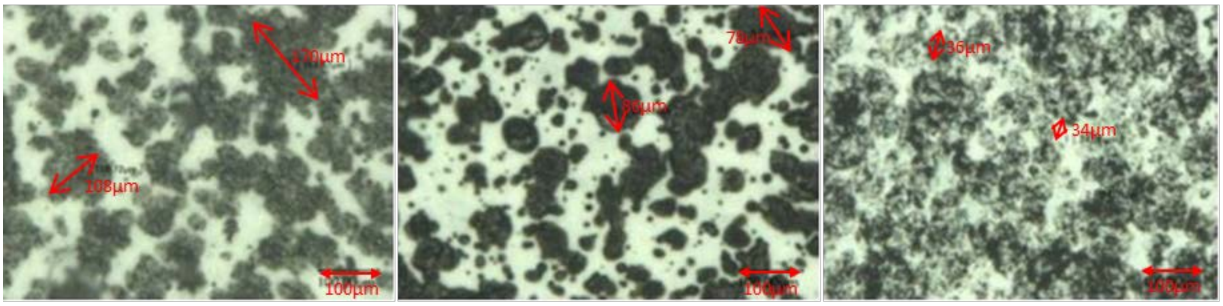

Figure 3: Microscopic measurement of speckle paintings; **left:** white powder and graphite; **middle:** modeling paint; **right:** titanium dioxide and black iron oxide

2.4 Evaluation and Calculation

After the test and the measurement, the definition of system parameters is critical for reasonable results. The first point is the size of the facets which is the number of pixels for one facet. The smaller the facets are the better the local resolution but the higher the risk of voids and measurement noise. The bigger one facet is, the worse is the detection of local effects. With the described surface preparation and the 2D setup a facet size down to 10x10pixels is possible and the needed measuring resolution as outlined in (2) is achievable.

The next step is the definition of the coordinate system, for a correct calculation of the strain, shear angle and further results. Within this work the x axis is in the tension direction, y is in plane of the specimen surface and z is the out of plane direction (not measured in 2D setups). The further evaluation and calculation depends highly on the specimen as each test needs special methods. Selected tests are discussed in the following chapter.

3. Measurement Results

Three different specimens have been tested and measured with the ARAMIS system. The first test is a scarf repaired adhesively bonded composite coupon. The aim is the detection of the effects of single plies on the bondline. The second test is also a scarfed bonded repair but in this case with an intended bondline flaw which effects on the specimen become clearly visible. The third results are taken from a crack lap shear specimen also with a very thin bondline where the shear angle of the adhesive is measured.

3.1 Bondline Strain Measurement in Scarfed Repaired Coupons

The main focus in this investigation is the bondline’s strain distribution and the effect of the different ply orientation. In Figure 4 the v. Mises strain plot for a load step close to the joint failure is shown. For a better orientation the right edge of the measurement area is not painted allowing the identification of the single ply position. In this specimen the scarf tip is on the upper right sight and runs down to the left. Due to the small area only 1/6 of the bondline length is visible.

The strain plot clearly shows the strain in the adhesive were 0° plies are in the laminate. Also a high strain in the 90° plies becomes visible which results in interlaminate cracks already before bondline failure. In the intersection between 0°, 90° plies and bondline the first indication of bondline failure

Excerpt from ISBN 978-3-00-053387-7

becoming visible. In further load steps crack growing in the 90° plies can be seen until the bondline fails.

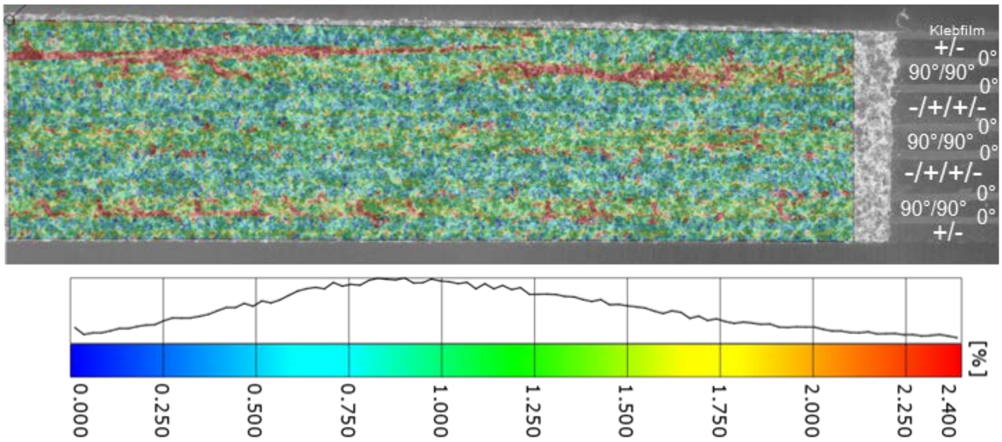

Figure 4: v Mises strain in scarf tip

3.2 Scarf Tip with Embedded Bondline Flaw and FEM Comparison

In this test the front view on a scarf tip of bonded repaired coupons was measured. As the intended measurement area is large enough, a 3D setup was used. To produce a defined flaw insight the bondline a PTFE foil was placed in the bonding area. Futhermore a detail FE Analysis was made with MSC Patran/Marc to calculate the strain and the effect of the flaw insight the bondline.

The result of the tension strain is plotted in Figure 5 for a load step just bevor failure. The top area is the parent material; the bottom is the repaired with the scarf tip. The influence of the flaw is clearly visible. For comparison to the FEA results a cut through the scarf end area, as illustrated in Figure 5, is given in Figure 6. The graph shows a strain concentration next to the flaw and nearly no strain within the flaw area. Additionally the results of the FEA are plotted. The FE results are the X component of the strain in the nodes next to the scarf end. The upper load level is just before failure, for both FEA and test, the second is around the half of the maximum FEA load.

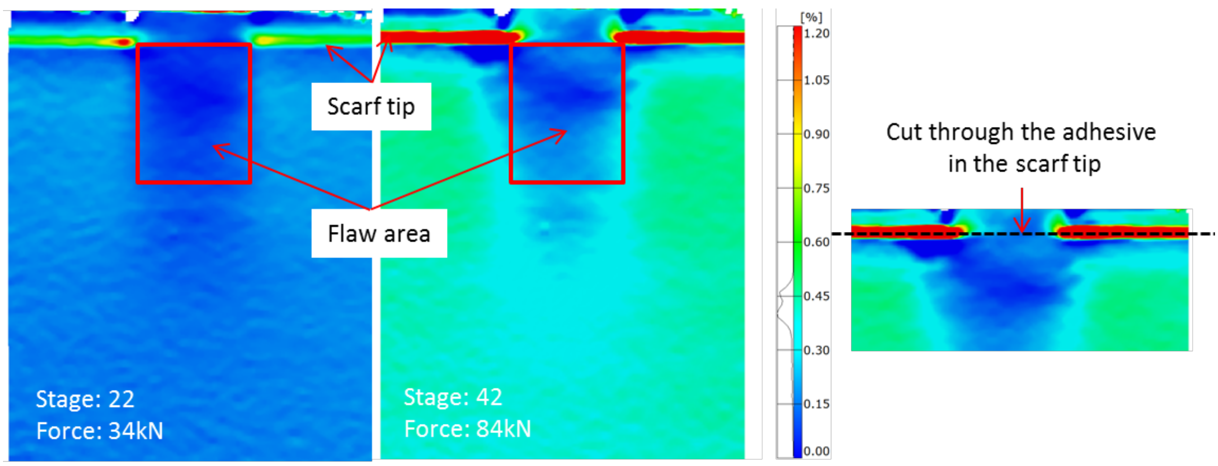

Figure 5: Epsilon x strain plot scarf repair with bondline flaw for two load steps [3]

Excerpt from ISBN 978-3-00-053387-7

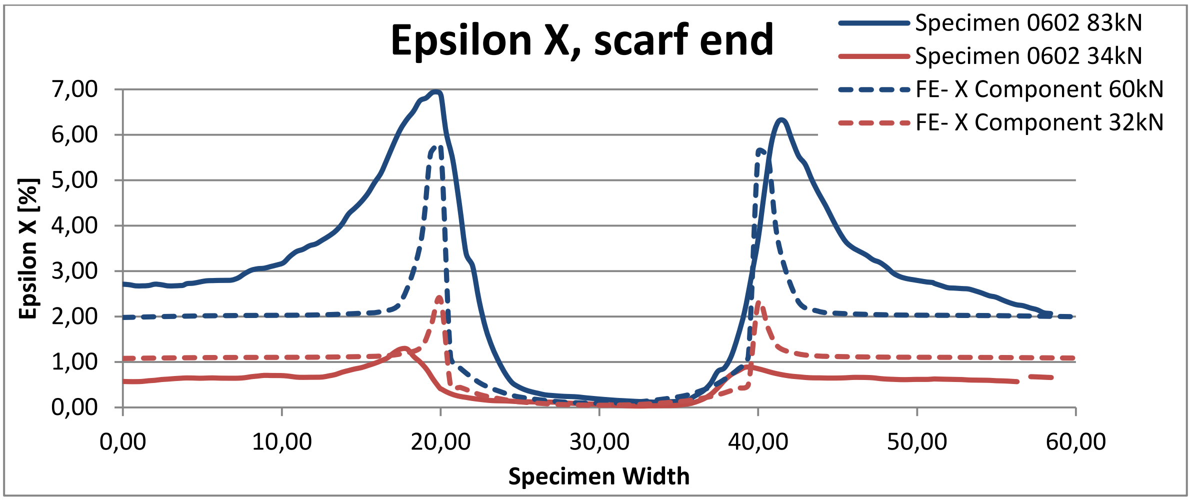

Figure 6: Epsilon x strain for cut through the scarf end, comparison between ARAMIS and FEM [3]

This plot confirms the interpretation made of the images above and verifies the results made in the FEM analyses. For the step just before failure the strain distribution over the specimen width is higher for the test results. The maximum area is similar compared to the FE results. But to mention is that the loads levels are slightly different. For a lower load step the FE results are slightly above the test results. But here the results are also very similar. For detailed results of bondline flaws on scarfed repairs see also [3].

3.3 Crack lap shear

Crack Lap Shear (CLS) coupon tests were undertaken as well. In CLS tests the shear angle and the propagation of the crack especially in the lap end are of interest. The ARAMIS measurement allows the determination of the shear angle with a high local resolution for the complete measurement area. In Figure 7 left the graph of the shear angle is plotted over the distance in the lap, starting on the left tip. In the right plot the shear angle is visualized on the specimen surface. The shear angle plot as well as the graph shows a high shear angle next to the Lap end of 3°. These results are used to validate FE calculations. [4]

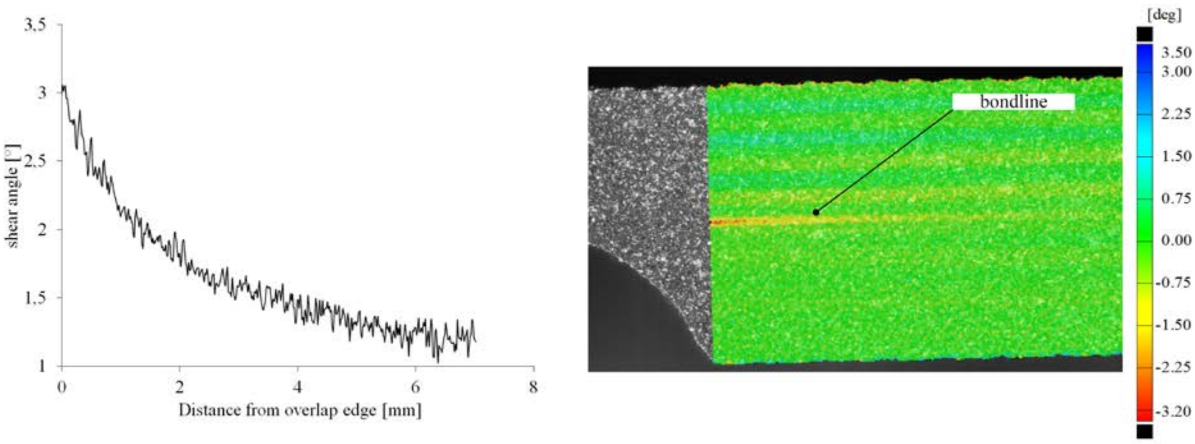

Figure 7: Measured shear angle along the bondline at 9.79kN tensile load [4]

Excerpt from ISBN 978-3-00-053387-7

4. Conclusions

The measurement results for different types of specimens clearly show that measuring with digital image correlation helps to get detailed information on the strain distribution within the specimens. This is essential for understanding anisotropic composite materials and adhesively bonded joints behavior and to validate FE models. With the improved lacquer techniques it is possible to produce repeatable and fast surface preparation. These combined with the right camera setup enable very small measurement volumes. Within these volumes the local resolution is high enough to get a detailed view on single composite plies and the bondline itself. The comparison to the undertaken FE simulations show good accordance of the test results from ARAMIS to the FE results.

References

[1] D.H. Mollenhauer, B.M. Fredrickson, G.A. Schoeppner, E.V. Iarve and A.N. Palazotto. Moiré interferometry measurements of composite laminate repair behavior: Influence of grating thickness on interlaminar response. *Composites: Part A, 39:1322–1330, 2008.*

[2] A. Spaggiari, E. Dragoni, and H.F. Brinson. Measuring the shear strength of structural adhesives with bonded beams under antisymmetric bending. *International Journal of Adhesion & Adhesives, 67 112-120, 2016.*

[3] J. Kosmann, D. Holzhüter, A.J. Gunnion and C. Hühne. Experimental and Finite Element Analysis of Bondline Flaw Criticality in Composite Scarf Joints. *Proceedings of the 16th European Conference on Composite Materials ECCM-16, Seville, Spain, June 22-26* 2014.

[4] T. Löbel, H. Sonnenberg, D. Holzhüter, C. Hühne. Fatigue evaluation and enhanced shear strain measurements of bonded composite joints. *10th International Conference on Composite Science and Technology, ICCST/10, Lisboa, Portugal 2.-4. September 2015.*

Excerpt from ISBN 978-3-00-053387-7